[21] T. J. Tarn and S. P. Yang, "Modeling and control for underwater robotic manipulators—An example," in *Proc. IEEE Int. Conf. Robotics and Automation*, Albuquerque, NM, Apr. 1997, pp. 2166–2171.
[22] L. L. Whitcomb and D. R. Yoerger, "Development, comparison, and preliminary experimental validation of nonlinear dynamic thruster models," *IEEE J. Oceanic Eng.*, vol. 24, pp. 481–494, Oct. 1999.
[23] D. R. Yoerger, J. G. Cooke, and J. J. Slotine, "The influence of thruster dynamics on underwater vehicle behavior and their incorporation into control system design," *IEEE J. Oceanic Eng.*, vol. 15, pp. 167–178, Jan. 1990.
[24] D. R. Yoerger and J. J. Slotine, "Robust trajectory control of underwater vehicles," *IEEE J. Oceanic Eng.*, vol. OE-10, pp. 462–470, Oct. 1985.
[25] J. Yuh, "Modeling and control of underwater robotic vehicles," *IEEE Trans. Syst., Man, Cybern.*, vol. 20, pp. 1475–1483, Nov./Dec. 1990.
[26] J. Yuh and M. West, "Underwater robotics," *J. Adv. Robot.*, vol. 15, no. 5, pp. 609–639, 2001.
[27] J. Yuh, S. Zhao, and P. M. Lee, "Application of adaptive disturbance observer control to an underwater manipulator," in *Proc. IEEE Int. Conf. Robotics and Automation*, Seoul, Korea, May 2001, pp. 3244–3248.
[28] W. H. Zhu, Y. G. Xi, Z. J. Zhong, Z. Bien, and J. De Schutter, "Virtual decomposition-based control for generalized high-dimensional robotic systems with complicated structure," *IEEE Trans. Robot. Automat.*, vol. 13, pp. 411–436, June 1997.

Model-Based Space Robot Teleoperation of ETS-VII Manipulator

Woo-Keun Yoon, Toshihiko Goshozono, Hiroshi Kawabe, Masahiro Kinami, Yuichi Tsumaki, Masaru Uchiyama, Mitsushige Oda, and Toshitsugu Doi

***Abstract*—In our previous research, we developed space robot teleoperation technology to achieve control from the ground of effective manual manipulations in orbit. To solve the communication time delay in the space robot teleoperation, we propose a mixed force and motion command-based space robot teleoperation system that is a model-based teleoperation. Moreover, we have also developed a compact 6-degree-of-freedom haptic interface as a master device. The important features of our teleoperation system are its robustness against modeling errors and its ability to realize the force exerted by the operator at the remote site. In this paper, we introduce a new control method, which modified our model-based teleoperation system, to control the real robotic system Engineering Test Satellite VII manipulator. Surface-tracking and peg-in-hole tasks have been performed to confirm the effectiveness of our system. The experimental results obtained with our system including the haptic interface demonstrate its ability to perform these tasks in space without any major problems. We also evaluated different master device approaches for the model-based space teleoperation system. For this purpose, we used two methods, which are a master–slave (MS) approach and a force-joystick approach. Our results show that the MS approach is the best control method for contact tasks in which the directions of motion of the slave arm and of the operator's input force are different, as in the surface-tracking task.**

***Index Terms*—Engineering Test Satellite VII (ETS-VII) manipulator, force feedback, force-joystick (FJ), haptic interface, master–slave (MS), model-based teleoperation, modeling error.**

I. Introduction

The International Space Station (ISS) is being constructed at present by many countries. Extra vehicular activity (EVA), in which an astronaut works in space, is necessary to construct such a space structure. However, the cost of launching astronauts in space is very high, and EVA presents many dangers. Thus, there is a demand for developing an autonomous space robot to work in space in the place of astronauts. However, it is difficult to develop a perfect autonomous space robot with the present robot technology. For this reason, the technology in which an operator on the ground teleoperates a semiautonomous space robot becomes important. The development of such a technology is especially important in Japan, which does not have, at the moment, the technology to launch astronauts in space by itself. In this context, the National Space Development Agency (NASDA) of Japan launched the Engineering Test Satellite VII (ETS-VII) in 1997 [1], [2]. The aim of the ETS-VII is the development of rendezvous docking and space robot technologies. Therefore, the 6-degree-of-freedom (DOF) manipulator and experiment equipment that can be operated by remote control from the ground is carried in the ETS-VII, and various experiments were conducted [3]–[6]. Several sensors and other equipment for the rendezvous docking are also carried in the satellite. Moreover, various real space robotic projects like the manipulator flight demonstration (MFD) have been conducted [7]. The Japanese experiment module (JEM), which is a part of the ISS, consists of four components, one of them being the JEM remote manipulator system (JEMRMS). The JEMRMS that is operated by the astronaut in the ISS will be used for experiments being conducted on the JEM or for supporting JEM maintenance tasks. In Germany, the space robot technology experiment (ROTEX) also has been conducted [8].

Communication time delay is one of the biggest problems encountered by teleoperation of a space robot from the ground. It is thought generally that a master-slave (MS) approach, where the position and force information of the slave system can be displayed to an operator, is an effective method of teleoperation. Until now, however, the MS approach has not been used in a space teleoperation system [7], [8], because the bilateral system generally becomes unstable due to the inherent communication time delay. This has made it impossible for the operator to definitely "feel" the force information in the few stable bilateral systems tested so far [9]–[11]. A model-based teleoperation system has been proposed [12], [13] to solve this problem, and a predictive display using virtual-reality techniques was also introduced [14]. In this system, the operator teleoperates the virtual model of both the space robot and the environment equipment. This virtual model is calculated by a ground-based computer. Therefore, the virtual model is the result of real-time simulation on the ground. The force and position information for the master arm are also calculated in the virtual world on the ground-based computer and can be stably and clearly displayed to an operator. In the space shuttle, where no time delay exists, a joystick that cannot display the force information is used as the master device. The joystick has been used in many space teleoperation projects like the ETS-VII and is also intended to be used in the ISS [2], [15], [16].

Manuscript received October 22, 2002; revised April 1, 2003. This paper was recommended for publication by Associate Editor Y. Liu and Editor I. Walker upon evaluation of the reviewers' comments.

W.K. Yoon is with the Intelligent Systems Institute, National Institute of Advanced Industrial Science and Technology (AIST), Tsukuba 305-8568, Japan (e-mail: wk.yoon@aist.go.jp).

T. Goshozono and T. Doi are with Toshiba Corporation, Tokyo 105-8001, Japan.

H. Kawabe and M. Uchiyama are with the Department of Aerospace Engineering, Tohoku University, Sendai 980-8579, Japan (e-mail: kawabe@space.mech.tohoku.ac.jp; uchiyama@space.mech.tohoku.ac.jp).

M. Kinami is with NS Solutions Corporation, Tokyo 104-8280, Japan.

Y. Tsumaki is with the Department of Intelligent Machines and System Engineering, Hirosaki University, Hirosaki 036-8561, Japan (e-mail: tsumaki@cc.hirosaki-u.ac.jp).

M. Oda is with the Japan Aerospace Exploration Agency, Tsukuba 305-8505, Japan (e-mail: oda.mitsushige@nasda.go.jp).

Digital Object Identifier 10.1109/TRA.2004.824700

The virtual world model as it is used in the above system, however, does not match exactly the real world. Precise model-matching methods have also been proposed [17], [18], however, it is impossible to completely remove modeling errors between the virtual and the real world.

Therefore, in our previous work, we have proposed a mixed force and motion command-based space robot teleoperation system that is robust against modeling errors [19]. It is a control method adding the error-robust character of its modeling to a control using both target force and target movement. Furthermore, we have also developed a new and a compact 6-DOF haptic interface to be used as a master arm [20]. The features of this haptic interface are a wide workspace and rapid motion ability. The haptic interface can display the force to the operator. Our teleoperation system and the haptic interface are connected via Ethernet. Therefore, they have a high potential for expandability, and they can be connected to other systems easily.

One feature of our method is that the tip velocity commands are generated by the forces exerted by the operator on the master device, by the motion information of the virtual arm [19]. The virtual arm shows simulation results which are calculated by the ground-based computer. The system also incorporates an automatic function to change between contact and noncontact modes. However, we are unable to manipulate the ETS-VII manipulator using velocity control, and to change the control modes between contact and noncontact for this manipulator. We should control this arm using the end-tip position only. Therefore, our teleoperation system cannot be used with the ETS-VII robot arm directly.

In this paper, we introduce a new control method that modifies our model-based teleoperation system. In our new system, the master and the virtual arms are controlled by the end-tip velocity. The slave arm on the ETS-VII is controlled by the end-tip position. The slave arm is also manipulated under compliance control. With the above modifications, our new system can retain the two important features that are its robustness against modeling errors, and its ability to realize the force exerted by the operator at the remote site.

In our experiments, surface-tracking and peg-in-hole tasks with and without artificially introduced modeling errors are performed in orbit. The effectiveness of our space teleoperation system is verified by carrying out the above tasks in a real space robotic system. The experimental results demonstrate that the surface-tracking task was carried out safely with and without artificially introduced modeling errors. The peg-in-hole task could also be carried out successfully though the operation with artificially introduced modeling errors became very complicated. We believe, therefore, that our teleoperation system can be applied easily to real space robotics, and that our system does have some level of robustness against modeling errors.

During the planning stage of the ETS-VII, a comparison between the joystick and the MS approaches was conducted, which included qualitative evaluations using a questionnaire submitted to the operators. We must, therefore, reevaluate the above controls quantitatively.

In this paper, the operability of the MS and the force-joystick (FJ) approaches is evaluated for the model-based space robotic teleoperation. Here, the FJ approach is a type of joystick approach using a force/torque sensor which may be better than the normal joystick approach, since the operator-exerted forces on the master device can become commands to the slave arm [21]. Thus, we perform the surface-tracking and the peg-in-hole tasks in order to evaluate the operability of the MS and FJ modes without artificially introduced modeling errors. From these results, we conclude that the MS mode appears to be the best control approach for contact tasks requiring different directions between the motion and the force of the slave arm, as in the surface-tracking task. Moreover, the MS and FJ modes are both suitable for tasks requiring the same directions for the motion and the force of the slave arm, as in the peg-in-hole task.

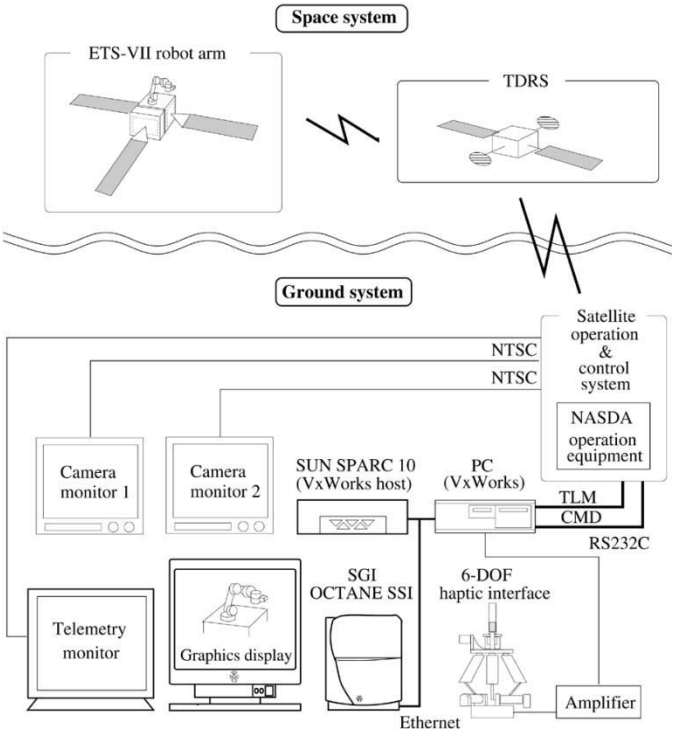

Fig. 1. Overview of the system.

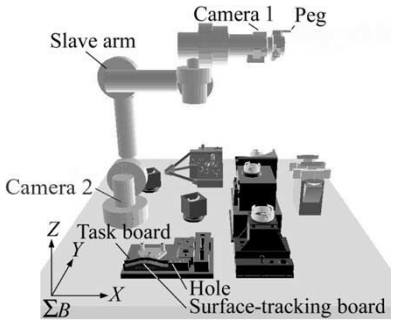

Fig. 2. Satellite-based slave system.

II. Experimental System

A. System Equipment

This experimental system consists of the space and the ground systems. An overview of the system is shown in Fig. 1. The space system is composed of the ETS-VII owned by NASDA and of the Tracking and Data Relay Satellite (TDRS) owned by the National Aeronautics and Space Administration (NASA). The equipment on the ETS-VII surface is shown in Fig. 2. Σ_B is the arm-based coordinate system. The ground system is composed of the NASDA satellite-operation system and of the operator-support system that was developed in our laboratory and is shown in Fig. 3. The operator-support system consists of a mixed force and motion command-based space robot teleoperation system and of a master controller that is a 6-DOF compact haptic interface. The command, which is generated in the operator-support system, is sent to the ETS-VII via the NASDA satellite-operation system and TDRS. The communication time delay in this communication loop is about 6 s. This time delay causes delay between the master arm and the slave arm. There is no time delay between the master arm and the virtual arm. This time delay is caused mainly by the total communication times between enormous computers on the ground. These computers are connected via a submarine cable between Japan and USA. This

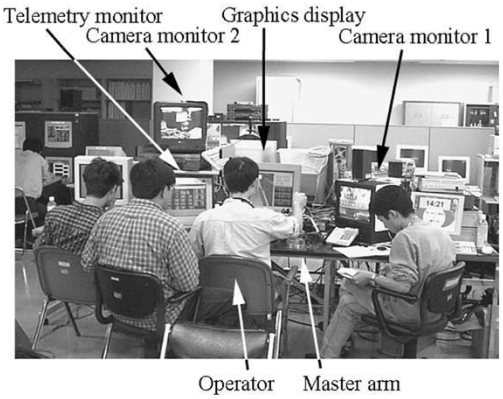

Fig. 3. Operator-support system.

time delay changes with the communication network load. To prevent any change in time delay, it is kept constant by buffering transceiver data beyond the time delay in the NASDA satellite-operation system.

The main components of this experimental system are as follows.

- Task board (TB)

  The TB, in Fig. 2, is mounted on the ETS-VII, and it carries various experimental equipment such as the surface-tracking board and the hole for peg-in-hole tasks, which are both used in this experiment. The shape of the surface-tracking board is that of a sinusoidal wave.
- Slave system

  The robotic arm mounted on the ETS-VII shown in Fig. 2 is a 6-DOF manipulator used as a slave arm [2]. Its overall length is about 2.4 m. The TB handling tool (TBTL) is attached to the tip of the manipulator, and an 18-mm diameter peg is installed at the tip of this handling tool. The experiments are performed using this peg and the TB. Two cameras are also attached at the end and at the first joint of this manipulator.
- Graphics computer

  An OCTANE SSI, manufactured by SGI (Mountain View, CA), is used as graphics computer, which displays the following information:

— virtual models of the slave arm (virtual arm) in solid graphics;
— virtual model of TB (virtual TB) in the solid graphics;
— reference tip position of the slave arm, which is sent to the ETS-VII, in the wire-frame model;
— numerical values of the tip positions and of the tip forces of the virtual arm;
— graphical user interface (GUI) for inputting control commands and parameters.

  A real image of this display is shown in Fig. 4. The reason for using the solid and the wire-frame models is given in detail in Section II-B. The concepts of virtual beam and virtual grip are used in these graphics for operator support [22], [23]. The operator can control the movement of the viewpoint and the scaling of the virtual model in these graphics.
- Master arm

  A compact 6-DOF haptic interface, shown in Fig. 5, is used as a common master device [20]. This means that the haptic interface is used as a master arm for both the MS and the FJ approaches. It comprises a small six-axis force/torque sensor to compensate for the nonbackdrivability of the high-ratio reduction gears. The master arm, the virtual arm, and the slave arm are commanded by the data of this force/torque sensor, which control the movements of the viewpoint in the virtual model, as well.

— MS approach

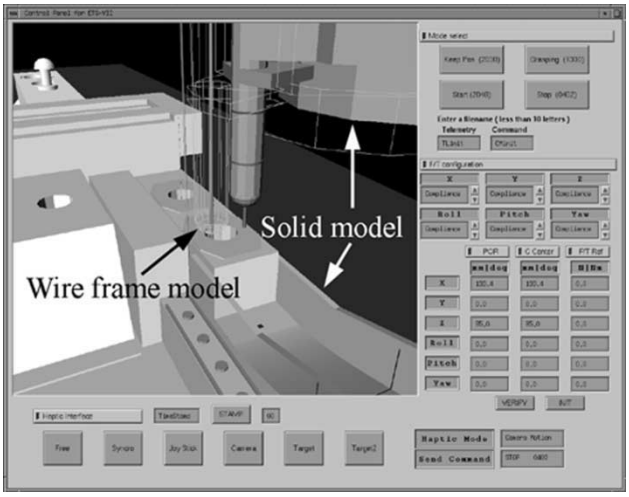

Fig. 4. Three-dimensional (3-D) graphics and GUI.

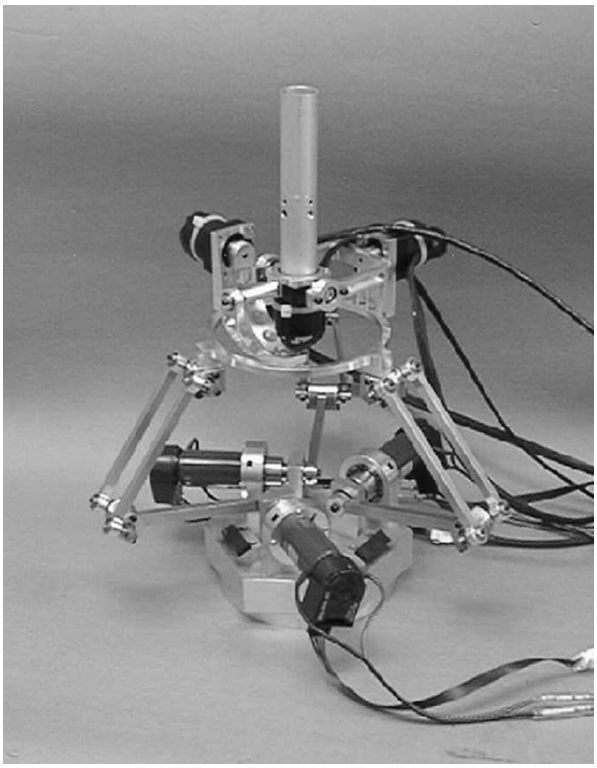

Fig. 5. 6-DOF haptic interface.

  The motions of both the virtual arm and the master arm (haptic interface device) are simulated exactly. Therefore, the operator can feel the force and the motion information of the slave arm through the master arm. If there are modeling errors, the motion of the master arm is different from that of the slave arm.

— FJ approach

  The FJ approach is a type of joystick approach using a force/torque sensor [21]. The master arm (haptic interface) is not moved at all, and only the force/torque sensor data are used to create the commands. The operator-exerted forces on the master arm can generate the commands to the virtual arm.

It is thought generally that the MS approach, where the position and force information of the slave arm can be displayed to an operator, is an effective method of teleoperation. Until now, the MS

approach has not been used in a space teleoperation system [7], [8], because the bilateral system generally becomes unstable due to the inherent communication time delay. A model-based teleoperation system has been proposed [12], [13] to solve this problem, and a predictive display using virtual-reality techniques was also introduced [14]. The FJ approach may be better than the normal joystick approach, since the operator-exerted forces on the master arm can become commands to the slave arm [21]. Then, in this paper, the operability of the MS and the FJ approaches is evaluated for the model-based space robotic teleoperation, and we estimate the possibility of the MS approach in the model-based space robot teleoperation.

- Main computer (VxWorks target computer)
  This computer controls the master arm, the virtual arm, and the slave arm. The communication to NASDA operating equipment is also done by this computer.
- Monitoring camera
  Two camera pictures of the slave arm are displayed on these monitors. Monitors 1 and 2 show images from the end-tip camera and from the first-joint camera of the slave arm, respectively, as shown in Figs. 2 and 3.
- Telemetry terminal display
  The numerical values of the positions and of the forces of the slave arm are displayed at this terminal.
- Software development computer (VxWorks host computer)
  The software used on the main computer is developed in this computer.

B. Control Methods

The main feature of our mixed force and motion command-based space robot teleoperation system is that the tip velocity commands are generated by the forces exerted by the operator on the master device, by the motion information of the virtual arm [19]. The system also incorporates an automatic function to change between contact and noncontact modes. For the manipulator on the ETS-VII, we cannot manipulate the velocity control and change the control modes between contact and noncontact. We should control this arm using the end-tip position only. Thus, in this experiment, the master and the virtual arms are controlled by the end-tip velocity, and the slave arm on the ETS-VII is controlled by the end-tip position. The slave arm is also manipulated under compliance control. With these control methods, the important features of our system, which are its robustness against modeling errors and its ability to realize the force exerted by the operator at the remote site, can be retained.

Here, the stiffness gains of the slave arm are 20 kg and 40 $\mathrm{kgm}^2/\mathrm{rad}$. The inertia gains are 2795 Ns/m and 2262 Nms/rad. The viscous gains are 200 N/m and 20 N·m/rad. We control translation only while orientation is fixed to that of the initial state. The maximum velocities at the tip of the master, the virtual arms and the reference position of the slave arm are set to 2.0 mm/s on the ground. However, the maximum velocity of the manipulator on the ETS-VII is set to 50.0 mm/s in the space system computer. These velocity limits are decided by NASDA for safety.

Transitions between contact and noncontact for the master and virtual arms depend only on specific conditions and the virtual environment. The slave arm is moved under compliance control. The maximum velocities of all these arms are set on the ground and the ETS-VII. Therefore, transitions between contact and noncontact of all arms will become stable.

The control methods of all these arms are as follows.

- Master arm
  - MS mode
    - Contact

$$\dot{x}_{\mathrm{m}} = k_f(f_{\mathrm{ref}} - f_{\mathrm{va}}) \tag{1}$$

    - Noncontact

$$\dot{x}_{\mathrm{m}} = k_v f_{\mathrm{ref}} \tag{2}$$

$$f_{\mathrm{ref}} = f_{\mathrm{m}} + k_d(\dot{x}_{\mathrm{va}} - \dot{x}_{\mathrm{m}}) + k_p(x_{\mathrm{va}} - x_{\mathrm{m}}) \tag{3}$$

  - FJ mode

$$\dot{x}_{\mathrm{m}} = k_{\mathrm{fj}}(x_{\mathrm{fj}} - x_{\mathrm{m}}) \tag{4}$$

- Virtual arm
  - MS and FJ modes
    - Contact

$$\dot{x}_{\mathrm{va}} = k_f(f_{\mathrm{m}} - f_{\mathrm{va}}) \tag{5}$$

    - Noncontact

$$\dot{x}_{\mathrm{va}} = k_v f_{\mathrm{m}} \tag{6}$$

- Slave arm

$$f_{\mathrm{sa}} = m_{\mathrm{sa}}\ddot{e} + c_{\mathrm{sa}}\dot{e} + k_{\mathrm{sa}}e \tag{7}$$

$$e = x_{\mathrm{s}} - x_{\mathrm{sa}} \tag{8}$$

$$x_{\mathrm{s}} = x_{\mathrm{va}} + \frac{f_{\mathrm{m}}}{k_{\mathrm{sa}}} \tag{9}$$

where the various terms of these equations have the following meaning:

x_{m}, x_{va}	tip position of the master and of the virtual arms, respectively;
x_{s}, x_{sa}	reference tip position and tip position of the slave arm, respectively;
x_{fj}	position bound on the master arm;
$\dot{x}_{\mathrm{m}}$, $\dot{x}_{\mathrm{va}}$	reference tip velocities of the master and of the virtual arms, respectively;
f_{m}	force/torque sensor data of the master arm;
f_{va}	virtual refraction/reaction force;
f_{ref}	position restraint force for the certification of the master arm backdrivability;
f_{sa}	force/torque sensor data of the slave arm;
k_v, k_f	velocity and force gains, respectively;
k_{fj}	restraint gains of the master arm;
k_p, k_d	position and damping gains for f_{ref}, respectively;
k_{sa}, m_{sa}, c_{sa}	stiffness, inertia, and viscous gains of the slave arm, respectively.

The block diagram of this system is shown in Fig. 6. Using (1)–(6), the master and the virtual arms are controlled by the operator's force. The force and motion information of the slave arm is not used in these controls. Then the virtual arm shows a predictive motion of the slave arm. The master and virtual arms is calculated in the ground-based computer only. There is no time delay between the master and the virtual arms. Therefore, the motion of both the master and the virtual arms are exactly simulated, hence, the operator can feel the tip movement of the virtual arm through the master arm. The change of modes between contact and noncontact is carried out automatically, achieving contact in the virtual world.

In general, a bilateral control is unstable under the communication time delay. In our model-based teleoperation system, however, all calculations and simulations are performed on the ground-based computer, and a feedfoward control is applied to the slave arm in our system. Thus, there is no time delay between the master arm and the virtual arm and time delay between the master arm and the slave arm. Then our system will be stable against the time delay.

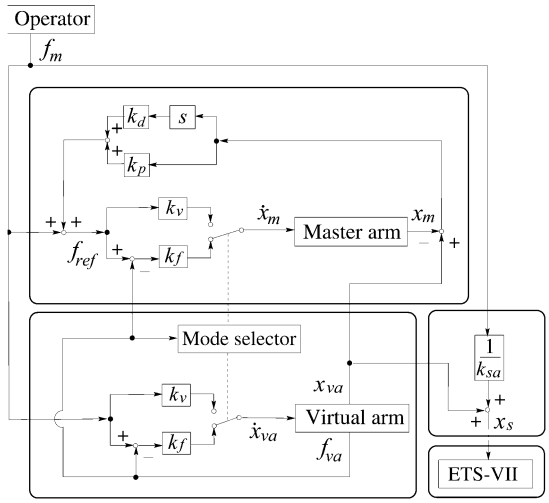

Fig. 6. Control block diagram of the system.

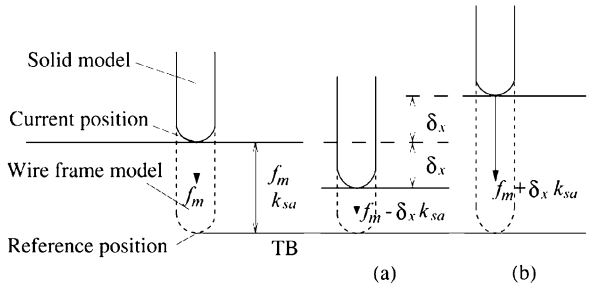

Fig. 7. Movement of the slave arm in a contact task.

The reference position of the slave arm (x_s) is calculated by the tip position of the virtual arm $(x_{\rm va})$, the force/torque sensor data of the master arm $(f_{\rm m})$, and stiffness gain of the slave arm $(k_{\rm sa})$ in (9).

Using (9), the slave arm can exert a force equal to the reference force $(f_{\rm m})$ if there are no modeling errors, since the slave arm is controlled in the compliance mode, as shown in Fig. 7. If there are modeling errors (δx), the normal model-based teleoperation cannot be executed. However, in our model-based teleoperation system, the slave arm can compensate for the modeling errors without generating large forces. For example, in Fig. 7(a), the force of the slave arm $(f_{\rm s})$ is given by

$$f_{\rm s} = f_{\rm m} - \delta x k_{\rm sa}. \tag{10}$$

In Fig. 7(b), the force of the slave arm $(f_{\rm s})$ is given by

$$f_{\rm s} = f_{\rm m} + \delta x k_{\rm sa}. \tag{11}$$

Using the above equations, in a noncontact task, the current position of the slave arm (solid model) is the same as that of the reference (wire-frame model). In a contact task, the current position of the slave arm (solid model) is different from that of the reference (wire-frame model). In order to distinguish between these positions, two types of graphics, the solid and the wire-frame models are required, as shown in Fig. 4.

Generally, the force that the operator inputs is unstable.One could expect the movement of the slave arm to become unstable when using the original force of the operator. However, it is not affected, since the tip-speed limitation of the reference position is 2.0 mm/s, and the sampling frequency of the input force from the operator is 2 Hz.

III. Details of the Experiments

The safety, effectiveness, and robustness against modeling errors of our teleoperation system and the operability in the MS and FJ modes of the model-based teleoperation system are evaluated in the following experiments.

In these experiments, we use the virtual model with and without artificially introduced modeling errors. The virtual model without artificially introduced modeling errors includes small modeling errors as it has been developed by the NASDA's experimental data and the draft of the ETS-VII. The virtual model with artificially introduced modeling errors includes a large modeling error compared with the virtual model without artificially introduced modeling errors. Moreover, all virtual models include dynamic modeling errors. The contents of the experiments are given below.

- Surface-tracking task

  The surface-tracking task is carried out using the peg at the tip of the TBTL and the surface-tracking board shown in Fig. 2.The length of the surface-tracking board is about 300 mm. At first, an operator applies a pressure on the peg of up to -20 N along the z direction while keeping it on the surface-tracking board. Once the operator has made contact with the peg, he/she checks the value of the force on the telemetry monitor and tracks the surface while maintaining this force. The details of the surface-tracking task are as follows.

  — Experiment 1-1

  The operator performs this task with the virtual model without artificially introduced modeling errors. This model is named "virtual model-1."

  — Experiment 1-2

  The operator performs this task with the virtual model with artificially introduced modeling errors of $+10$ mm in both the x and the z directions. This model is named "virtual model-2."

  In experiment 1-2, the operator already knows the value of artificially introduced modeling errors before executing the task.

- Peg-in-hole task

  The peg-in-hole task is also carried out using the setup shown in Fig. 2. The peg and the hole diameters are 18.0 and 18.4 mm, respectively. The start position is $+10$ mm in the x direction, -18 mm in the y direction, and $+21$ mm in the z direction, measured from the center of the hole, respectively. The details of the peg-in-hole task are as follows.

  — Experiment 2-1

  The operator performs this task with the same virtual model-1 as in Experiment 1-1.

  — Experiment 2-2

  The operator performs this task with the virtual model having artificially introduced modeling errors of $+5$ mm in the x direction and $+10$ mm in the z direction, respectively. This model is named "virtual model-3."

  In Experiment 2-2, the operator knows that artificial modeling errors have been introduced, but does not know the scale of these errors before executing the experiment.

One master arm and four displays, shown in Fig. 3, are set up in the operator-support system. The motion area of the slave arm is very small in this experiment. The parts of the slave arm do not collide with the experiment equipment on the ETS-VII. Therefore, it is not necessary for the operator to check monitor 2, thus, he/she teleoperates with one master arm and three displays. The visual information seen by the operator is described as follows:

- ①: Virtual arm and the virtual TB at the graphics display;
- ②: Numerical information of the virtual-arm tip position at the graphics display;
- ③: Numerical information of the virtual-arm tip force at the graphics display;
- ④: Numerical information of the slave-arm tip position at the telemetry monitor;

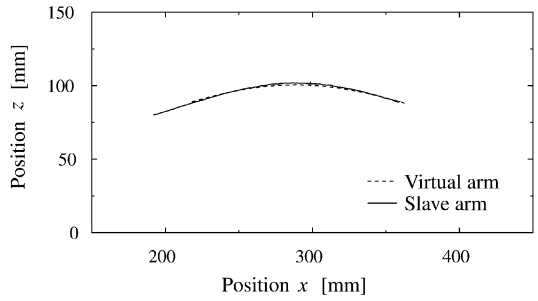

Fig. 8. Surface-tracking task without artificially introduced modeling errors.

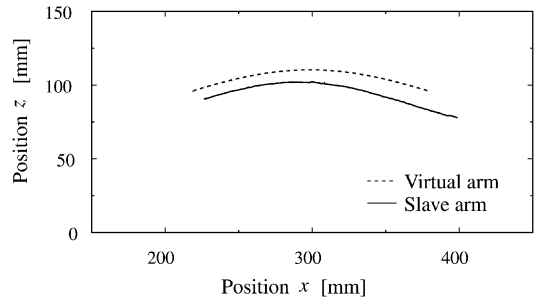

Fig. 9. Surface-tracking task with artificially introduced modeling errors.

- ⑤: Numerical information of the slave-arm tip force at the telemetry monitor;
- ⑥: Picture of the end-tip camera of the slave arm at camera monitor 1.

To confirm the information used by the operator during the experiments, we recorded the operator's visual activity with the video camera.

The above tasks were performed once for each mode by only one operator because we were required to use the real space robot of the ETS-VII, and experimental time is limited.

IV. Results of the Experiments

A. Surface Tracking

The results of Experiments 1-1 and 1-2 are shown in Figs. 8–11, respectively. These experiments were executed in the MS mode. The results of Experiment 1-1 executed using the FJ mode are shown in Fig. 12. We can observe geometry modeling errors of a few millimeters in the peg trajectory in Fig. 8. We can also observe the effects of artificially introduced modeling errors on the peg trajectory in Fig. 9. When the operator applies a pressure on the peg up to -20 N along the z direction, the difference between the reference position and the virtual arm is 100 mm in the z direction. The force creating a deviation, due to the modeling errors of $+10$ mm in the z direction, is 2 N in Fig. 9.

In each experiment, movements in only one direction are studied because the available experimental time is limited. The start and the end points are different in Figs. 10–12. However, the difference in start points does not affect the operator sensations, since the operator changes viewpoint in the virtual model and always pulls the master arm from a far point toward his/her breast.

The value of the force of the operator on the master arm is zero for some time in these figures. This corresponds to the operator changing the viewpoint of the virtual world. In our teleoperation system, the master arm is used for slave-arm manipulation and for the viewpoint manipulation. Therefore, we set $f_{\mathrm{m}} = 0$ in (3), (5), (6), and (9) while the operator is changing the viewpoint. During this time, the reference position of the slave arm keeps a constant value.

First, we will discuss the effectiveness of our space teleoperation system.

In Figs. 10 and 11, the x and the z positions of the virtual and the slave arms deviate a little when moving up the surface and much more when moving down. The reasons for this situation are the shape of the surface-tracking board, the relative positions of the corresponding arms, the velocity limits of the two arms and a frictional force of the dynamics modeling errors ignored in the virtual model. The peg positions of the virtual and the slave arms, and the reference position of the slave arm, are shown in Fig. 13. While moving up the surface, all these arms move at 2.0 mm/s. While changing the viewpoint, the virtual arm and the reference position of the slave arm are locked. The slave arm, however, keeps moving toward the reference position. Therefore, the slave arm passes by the current position of the virtual arm. While moving down the surface, the frictional force against the slave arm is very small because the reaction force of the slave arm is small, hence, the actual force working to create the motion of the slave arm becomes large. Therefore, the slave arm can move at a velocity over 2.0 mm/s because its limit is set at 50.0 mm/s in the ETS-VII computer. However, the virtual arm's motion is limited to 2.0 mm/s. Therefore, the virtual arm remains at 2.0 mm/s. As a result, the error of position between the slave and the virtual arms increases during this part of the motion.

In Figs. 10 and 11, the x direction force of the slave arm is very different from that of the master arm. This situation is due to psychological effects on the operator, the shape of the surface-tracking board, and the velocity limit of both the master arm and the reference position for the slave arm. We will first describe the master arm in detail. Before starting the surface-tracking task, both the slave and the virtual arms stop while the master arm is exerting a force of -20 N against the surface in the z direction. When the surface-tracking task starts, the operator exerts a large force in the x direction to move both arms. Therefore, the master arm generates a large reaction force. The same situation occurs after changing viewpoint. The operator maintains a large force during this task because the velocity limit of the master arm is very small. The master arm is pressed in the x direction only, since the operator should keep the direction of the force constant for moving the master and the slave arms in the positive x direction. We will now describe the slave arm using Fig. 13. While moving up the surface, the right side of the slave arm's peg is in contact with the surface, whereas, it changes to the left side when it moves down the surface. Therefore, the sign of the slave arm's force in the x direction changes when the motion along the surface changes from the upward to downward.

In Fig. 10, the master and the slave arm reach the target force, which is -20 N. In Fig. 11, the master arm always exerts a force of -20 N in the z direction. The slave arms reaches -20 N in the z direction while moving up the surface. However, this force decreases while moving down the surface. This is why the slave arm continues to move down the surface.

These results show that this task could be performed successfully without generating any large forces that could disturb the execution of Experiments 1-1 and 1-2. Therefore, we can confirm the effectiveness and robustness against modeling errors of our teleoperation system for the surface-tracking task.

We will discuss now the operability of the MS and FJ modes.

In the MS and FJ modes, the control commands are generated from the force/torque data of the master arm. Here, we compare the forces of the master and slave arms in the MS and FJ modes. The profiles of both the virtual arm's position and the slave arm's position are almost coincident in the two modes, as shown in Figs. 10 and 12. The profiles of the slave arm's forces are also similar in both modes. The standard deviations for the z direction force of both the master arm and the slave arm in the experiment are shown in Fig. 14. The standard deviations of the master arm are clearly smaller in the MS mode than in the FJ

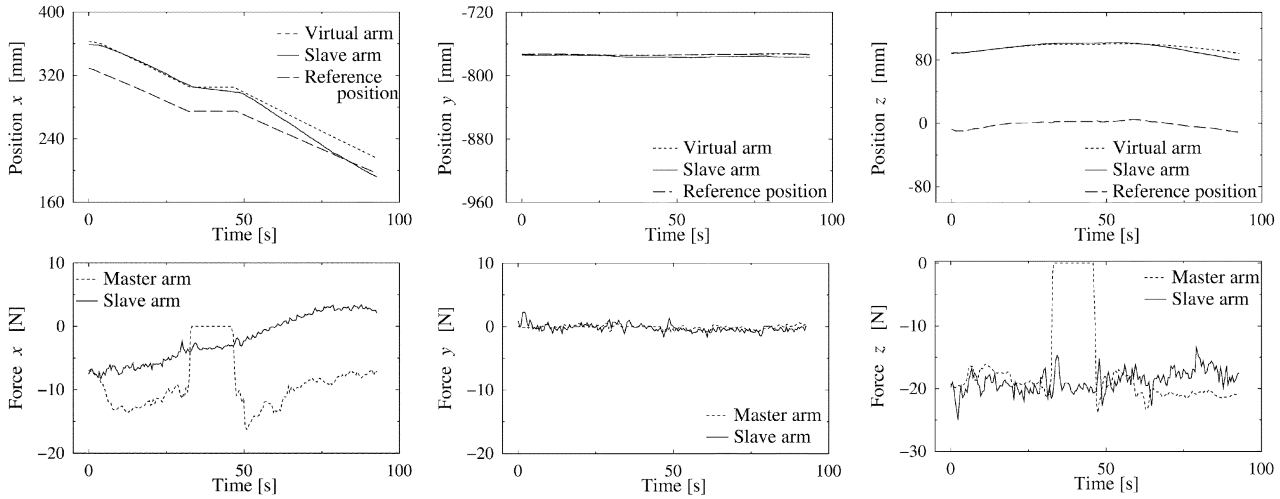

Fig. 10. Surface-tracking task without artificially introduced modeling errors in the MS mode.

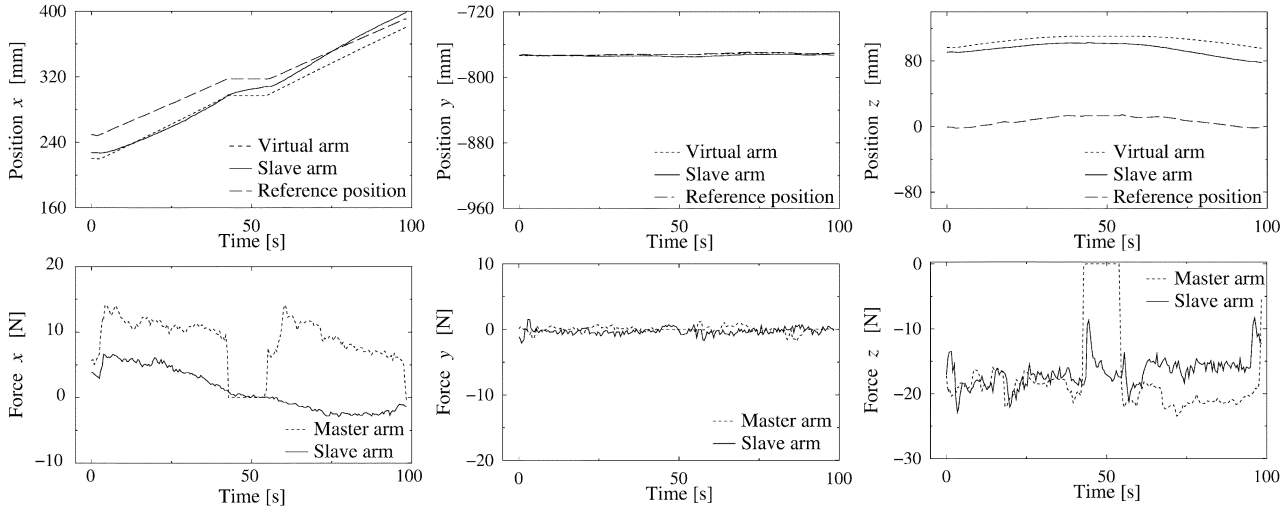

Fig. 11. Surface-tracking task with artificially introduced modeling errors in the MS mode.

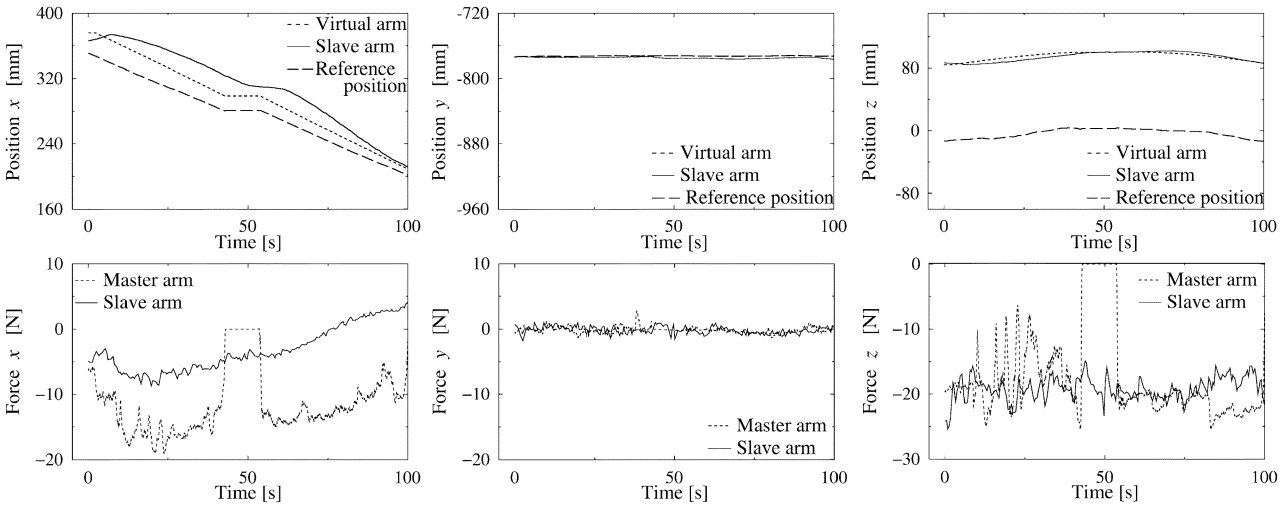

Fig. 12. Surface-tracking task without artificially introduced modeling errors in the FJ mode.

mode. The standard deviations of the slave arm are a little smaller in the MS mode than in the FJ mode. Table I gives the number of times the operator used visual information and his/her information acquisition time (in seconds) for both modes. In the surface-tracking experiment, the operator does not use information ② and ④. We believe that the reasons for this are that the operators do not need information ②, since

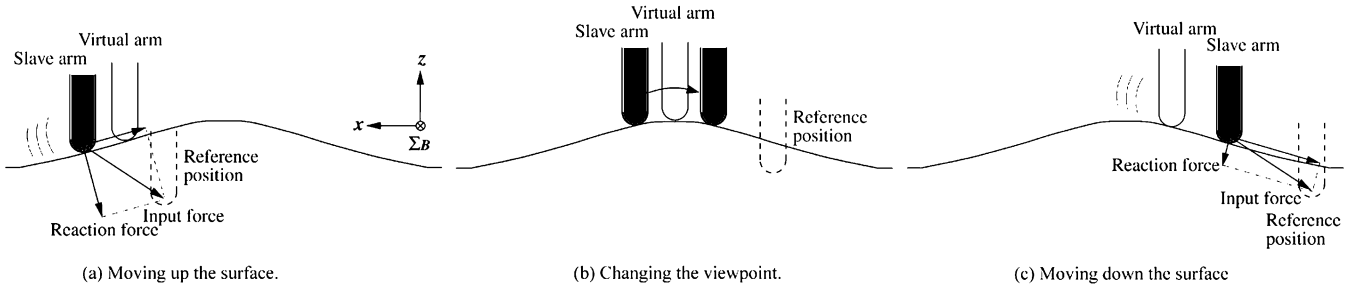

(a) Moving up the surface. (b) Changing the viewpoint. (c) Moving down the surface

Fig. 13. Relation to the virtual arm, the slave arm, and the reference position of the slave arm.

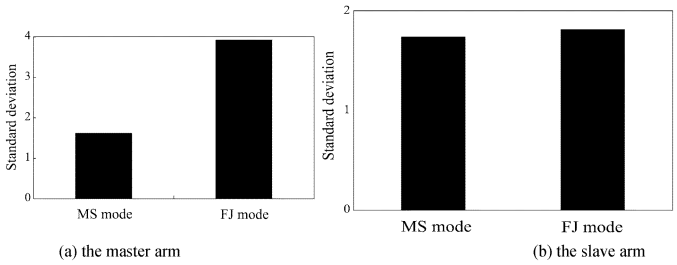

(a) the master arm (b) the slave arm

Fig. 14. Average standard deviations for the z direction force in the surface-tracking task.

TABLE I
VISUAL INFORMATION USED DURING SURFACE-TRACKING TASK

	MS mode		FJ mode	
	Times	Time [s]	Times	Time [s]
① Graphics	14	74.5	25	76.5
③ Numerical virtual force	8	8.5	15	8.0
⑤ Numerical real force	4	4.0	5	3.0
⑥ Real Video	3	3.0	3	2.5
Total	29	90.0	48	90.0

the position of the virtual arm is displayed on the graphics, and that the operator can not recognize intuitively the position of the slave arm from information ④. In the following discussion, the results of these two information are omitted. Information ① is the most used information in the MS and FJ modes. However, in the FJ mode, information ② is used as much as information ①. According to Table I, the number of times the operator acquired information from ① and ③ is larger in the FJ mode than in the MS mode. However, the acquisition times in both modes are almost equal. Therefore, we conclude that in the FJ mode, the operator teleoperated while quickly changing from one visual information to the other.

We describe now the motion and the force directions of both the master and the slave arms in the surface-tracking task. Fig. 13 shows the motion of the slave arm and the input force direction. While moving up the surface, the operator should pull the slave arm up in the z direction and exert the force along the negative z direction at the same time. We describe the details in each mode as follows.

- MS mode

  The operator can get information about both the direction of the slave arm and the direction of the force exerted by the master arm.Therefore, he/she can easily adjust the input force direction.
- FJ mode

  The operator cannot get information about the direction of motion of the slave arm through the master arm. Therefore, the standard deviation of the master arm's force becomes larger than that in the MS mode.

From these results, we could conclude that the MS mode is suitable for contact tasks in which the direction of motion of the slave arm is different from that of the operator's input force command.

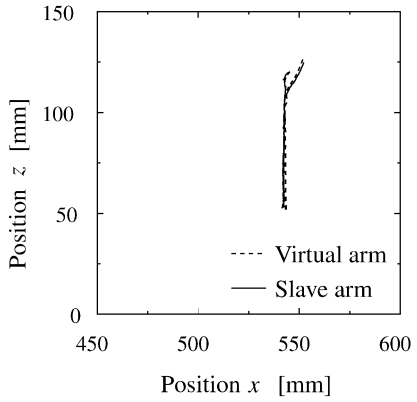

Fig. 15. Peg-in-hole task without artificially introduced modeling errors.

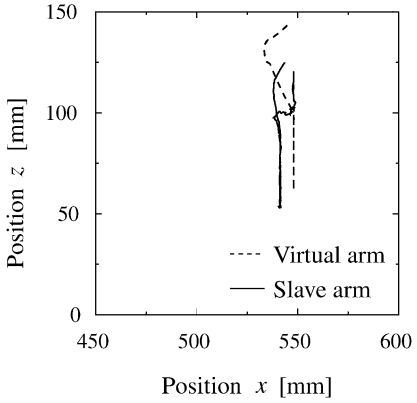

Fig. 16. Peg-in-hole task with artificially introduced modeling errors.

B. Peg-In-Hole

The results of Experiments 2-1 and 2-2 are shown in Figs. 15–18, respectively. These experiments are executed in the MS mode. The results of Experiment 2-1 executed using the FJ mode are shown in Fig. 19. We can observe a few millimeters of geometry modeling errors in the peg trajectory in Fig. 15. We can observe the presence of artificially introduced modeling errors in the peg trajectory in Fig. 16.

First, we will discuss the effectiveness of our space teleoperation system.

In Experiment 2-1, the position of the virtual arm is the same as that of the slave arm; the slave arm does not generate a large force, as shown

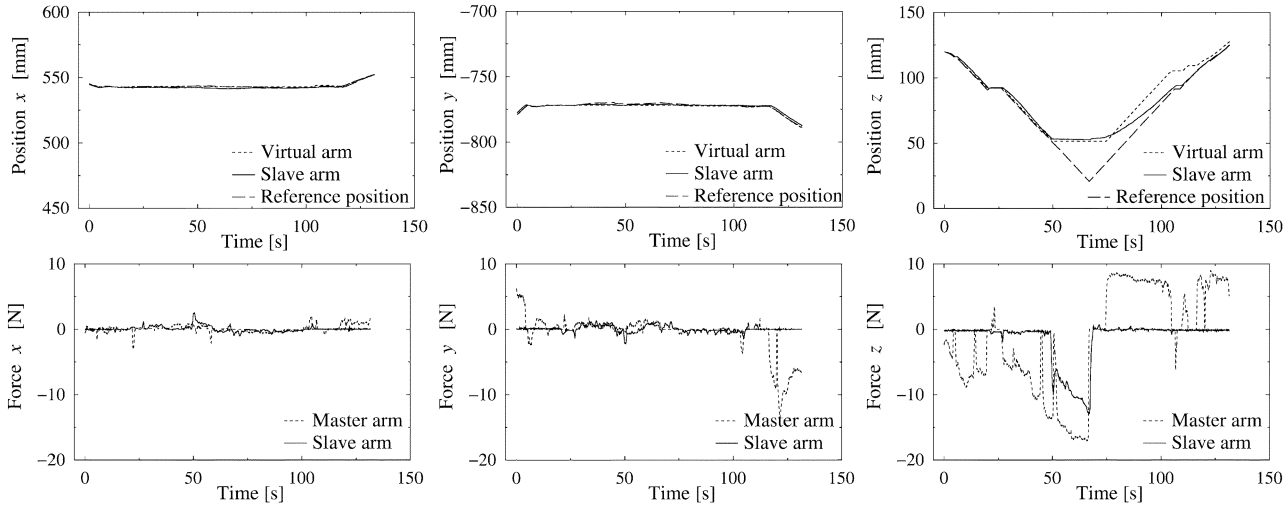

Fig. 17. Peg-in-hole task without artificially introduced modeling errors in the MS mode.

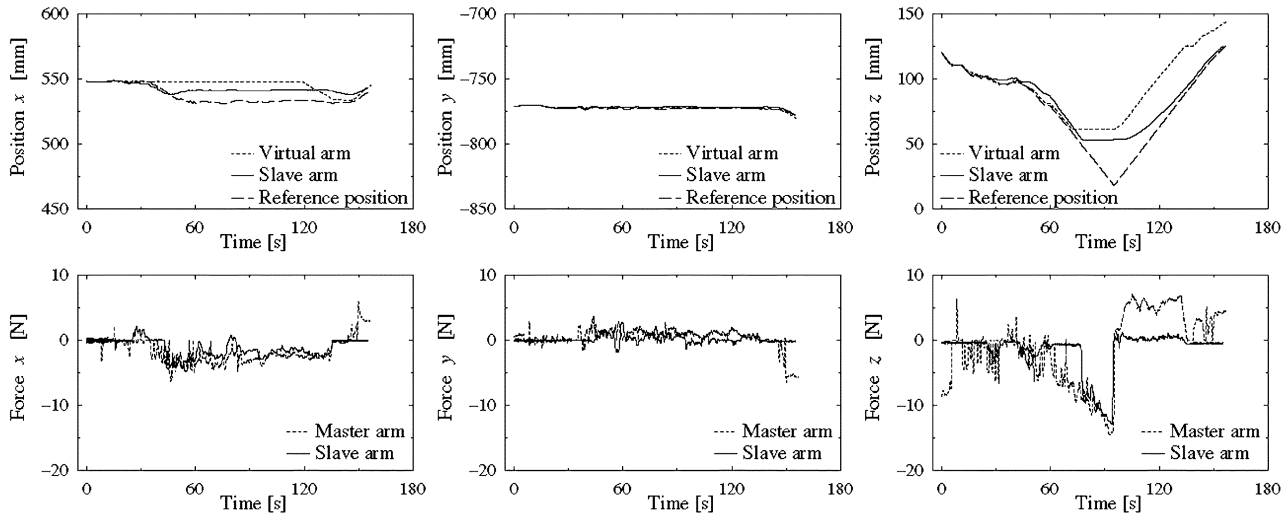

Fig. 18. Peg-in-hole task with artificially introduced modeling errors in the MS mode.

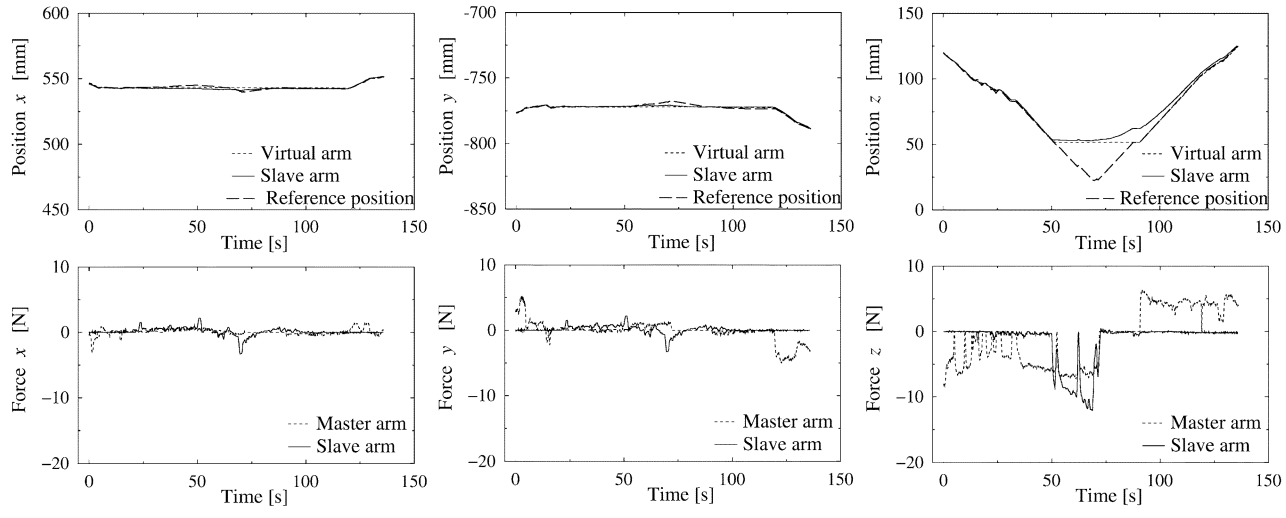

Fig. 19. Peg-in-hole task without artificially introduced modeling errors in the FJ mode.

in Figs. 15 and 17. This task is performed smoothly. The procedure for this task is as follows.

- 0–25 s: The peg is moved to the right to come above the hole in free space.
- 25–50 s: The peg is inserted into the hole.
- 50–75 s: The operator exerts a force of -5 N in the z to confirm that the peg is inserted.
- 75–100 s: The peg is pulled up.

TABLE II
VISUAL INFORMATION USED DURING PEG-IN-HOLE TASK

	MS mode		FJ mode	
	Times	Time [s]	Times	Time [s]
① Graphics	24	97.0	35	77.0
③ Numerical virtual force	4	2.5	4	3.0
⑤ Numerical real force	17	32.0	27	36.0
⑥ Real video	7	5.5	14	16.0
Total	52	137.0	80	132.0

- 100 s: The peg is moved to the end point in free space.

In Experiment 2-2, the operator is aware of the presence of artificially introduced modeling errors in the virtual model but does not know the amplitude, the type, and the number of modeling errors introduced. Therefore, the operator has to teleoperate carefully.

- 0–15 s: The peg is moved right above the hole in the virtual world.
- 15–25 s: The peg of the virtual arm is inserted a little into the virtual TB. However, as the force of the slave arm is generated in the z direction, the operator notices that the slave arm cannot insert the peg in the hole.
- 25–45 s: The operator starts searching for the hole in the real world. $f_{\rm m}/k_{rmsa}$ which is the second term on the right-hand side of (9) is used for this purpose. When the virtual peg is inserted a little into the hole of the virtual TB, the operator inputs the x and y forces and controls the wire-frame model, shown in Fig. 4, for the hole search. During this time, the virtual and the master arms hardly move. During the search, the z direction force of the slave arm is quite high. If the slave arm can reach the hole and insert the peg in it, this force will go to zero. Therefore, the operator keeps on searching, monitoring only the z direction force. This situation is shown in Fig. 18.
- 45 s: The operator discovers the spot where the z direction force becomes equal to zero and decides that this might be the position of the hole.
- 45–65 s: The operator inserts the virtual peg into the virtual hole. At the same time, the wire-frame model also moves to get into the hole, maintaining its position where the hole was discovered, and the operator inserts the slave peg into the real hole.
- 65–85 s: In order to confirm the complete peg insertion, the operator exerts a force on the peg larger than 5 N.
- 85–125 s: The peg is pulled out.
- 125 s: The peg is moved to the end point in free space.

The peg-in-hole task could be performed very easily in Experiment 2-1. Although the operation became quite complicated in Experiment 2-2, the operator could carry out the task successfully without generating large disturbing forces. From these results, we can confirm the effectiveness and robustness against modeling errors of our teleoperation system for the peg-in-hole task.

We will discuss now the operability of the MS and FJ modes.

Table II gives the number of times the operator used visual information and his/her information acquisition time (in seconds) for both modes. According to Figs. 17 and 19, the profiles of both the virtual arm's position and the slave arm's position are coincident in both modes. However, the operator input force in the FJ mode is smaller than the one used in the MS mode. The reason for this is that the operator inputs a small force to ensure the force is not too large, since the experiment in the FJ mode is executed before the one in the MS mode. Therefore, we can say that the difference in the operability of the MS and FJ modes is not apparent from Figs. 17 and 19. According to Table II, information ③ is used only a few times, since it is not necessary to keep a constant force. In contrast, information ⑤ is used many times to check the very large force in the real motion. The number of times the operator acquired information is larger in the FJ mode than in the MS mode. The reason for this is also that the operator inputs a small force to ensure the force is not too large, since the experiment in the FJ mode is executed before the one in the MS mode. Therefore, it can be concluded that the difference in the operability of the MS and FJ modes is not apparent from Table II, as well. We speculate that these differences are generated by the fact that the first experiment is performed in the FJ mode and the second one in the MS mode for the operator to execute the peg-in-hole task using the real space robot.

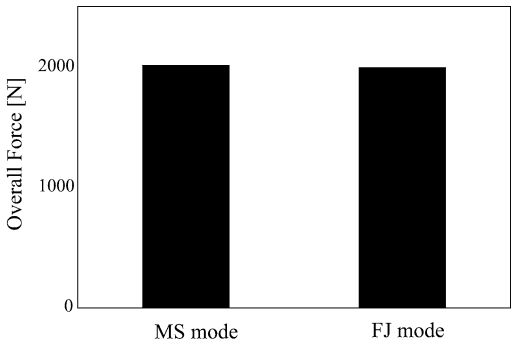

Fig. 20. Overall contact force of the slave arm for the z direction in the peg-in-hole task.

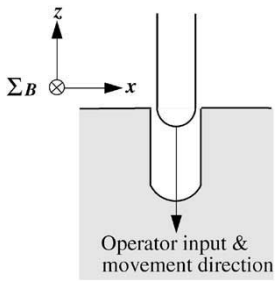

Fig. 21. Motions and force in the peg-in-hole task.

In order to compare the generated forces developed by the slave arm in the z direction, the overall absolute values in all the peg-in-hole experiments are shown in Fig. 20. These values are very similar in both modes.

We describe now the motion and the force directions of both the master and the slave arms in the peg-in-hole task. Fig. 21 shows the direction of motion of the slave arm and the input force direction. The approach to the hole is a free-space motion. Therefore, no significant differences appear in the two modes. During peg insertion, the direction of motion of the slave arm and the input force direction are the same. For this reason, the operator can easily adjust the input force direction along the hole surface, whether he/she obtains the motion information of the slave arm from the master arm or not. Therefore, we conclude that no significant differences appear among these modes, even in this process.

From these results, we can conclude that there is almost no difference between the MS and FJ modes for the tasks in which the direction of motion of the slave arm is the same as that of the input force.

V. CONCLUSIONS

In this paper, we introduced a new control method that modified our model-based teleoperation system against the time delay, and this

method was applied to the ETS-VII manipulator teleoperation in orbit. A compact haptic interface was used as a master device in our ETS-VII robot arm teleoperation experiments.

We performed surface-tracking and peg-in-hole tasks with and without artificially introduced modeling errors with a real manipulator in orbit with the communication time delay. The surface-tracking task was carried out safely with and without artificially introduced modeling errors. The peg-in-hole task could also be carried out successfully, though the operation with artificially introduced modeling errors became very complicated.

These results confirm that our new teleoperation system can be applied easily to real space robotics, and that this system does have some level of robustness against modeling errors and of stable against time delay.

Moreover, we performed the surface-tracking and the peg-in-hole tasks in order to evaluate the operability of the MS and FJ modes without artificially introduced modeling errors in the model-based teleoperation. We used both the motion and force information from all arms for this evaluation. We also used the visual information acquired by the operator for this evaluation. According to our results, the MS mode appears to be the best control approach for contact tasks requiring different directions between the motion and the force of the slave arm, as in the surface-tracking task. Moreover, the MS and FJ modes are both suitable for tasks requiring the same directions for the motion and the force of the slave arm, as in the peg-in-hole task.

REFERENCES

[1] M. Oda, "In-orbit experiment of space robot technologies on ETS-7," *J. Robot. Mechatron.*, vol. 6, no. 5, pp. 370–374, 1994.

[2] ——, "Space robot experiments on NASDA's ETS-VII satellite: Preliminary overview of the experiment results," in *Proc. IEEE Int. Conf. Robotics and Automation*, Detroit, MI, 1999, pp. 1390–1395.

[3] K. Matsumoto, S. Wakabayashi, L. Penin, M. Nohmi, H. Ueno, T. Yoshida, and Y. Fukase, "Teleoperation control of ETS-7 robot arm for on-orbit truss construction," in *Proc. i-SAIRAS'99*, Nordvijk, The Netherlands, 1999, pp. 313–318.

[4] S. Kimura, S. Tsuchiya, Y. Nagai, K. Nokamura, K. Satoh, and H. Morikawa, "Teleoperation experiments for antenna assembling experiment on Engineering Test Satellite VII," in *Proc. 9th Int. Conf. Advanced Robotics*, Tokyo, Japan, 1999, pp. 331–339.

[5] K. Landzettel, B. Brunner, K. Deutrich, G. Hirzinger, G. Schreiber, and B. M. Steinmetz, "DLR's experiments on the ETS VII space robot mission," in *Proc. 9th Int. Conf. Advanced Robotics*, Tokyo, Japan, 1999, pp. 347–353.

[6] T. Imaida, Y. Yokokohji, T. Doi, M. Oda, and T. Yoshikawa, "Ground-space bilateral teleoperation experiment using ETS-VII robot arm with direct kinesthetic coupling," in *Proc. IEEE Int. Conf. Robotics and Automation*, Seoul, Korea, 2001, pp. 1031–1038.

[7] M. Nagatomo, C. Harada, Y. Hisadome, M. Ikeuchi, M. Tanaka, Y. Tanaka, H. Yamamuro, Y. Uchibori, and K. Imaki, "Operation of crew-tended space robot in MFD" (in Japanese), in *Proc. 41th Space Sciences and Technology Conf.*, Hokkaido, Japan, 1997, pp. 97–15–11.

[8] G. Hirzinger, B. Brunner, J. Dietrich, and J. Heindl, "Sensor-based space robotics-ROTEX and its telerobotic features," *IEEE Trans. Robot. Automat.*, vol. 9, pp. 649–663, Oct. 1993.

[9] W. R. Ferrel, "Delayed force feedback," *IEEE Trans. Human Factors Electron.*, vol. HFE-8, pp. 449–455, 1966.

[10] G. Niemeyer and J. E. Slotine, "Stable adaptive teleoperation," *IEEE J. Ocean. Eng.*, vol. 16, pp. 152–162, 1991.

[11] R. J. Anderson and M. W. Spong, "Asymptotic stability for force-reflecting teleoperators with time delay," *Int. J. Robot. Res.*, vol. 11–2, pp. 135–149, 1992.

[12] S. Tachi and T. Sakaki, "Impedance controlled master-slave manipulation system. Part I. Basic concept and application to the system with a time delay," *Adv. Robot.*, vol. 6, no. 4, pp. 483–503, 1992.

[13] T. Kotoku, "A predictive display with force feedback and its application to remote manipulation system with transmission time delay," in *Proc. IEEE/RSJ Int. Conf. Intelligent Robotics and Systems*, Raleigh, NC, 1992, pp. 239–246.

[14] M. V. Noyes and T. B. Sheridan, "A novel predictor for telemanipulation through a time delay," in *Proc. Annu. Conf. Manual Control*, Moffett Field, CA, 1984.

[15] K. Wakata, "Teleoperation on onboard robot arm on ETS-VII and robotic for manned space system" (in Japanese), *J. Robot. Soc. Japan*, vol. 17–8, pp. 1096–1101, 1999.

[16] M. Oda, "System engineering approach in designing the teleoperation system of the ETS-VII robot experiment satellite," in *Proc. IEEE Int. Conf. Robotics and Automation*, Albuquerque, NM, 1997, pp. 3054–3061.

[17] E. Oyama, N. Tsunemoto, S. Tachi, and Y. Inoue, "Remote manipulation using virtual environment," in *Proc. 2nd Int. Symp. Measurement and Control in Robotics*, Tsukuba, Japan, 1992, pp. 311–318.

[18] W. S. Kim, D. B. Genney, and E. C. Chalfant, "Computer vision assisted semiautomatic virtual reality calibration," in *Proc. IEEE Int. Conf. Robotics and Automation*, Albuquerque, NM, 1997, pp. 1335–1340.

[19] Y. Tsumaki and M. Uchiyama, "A model-based space teleoperation system with robustness against modeling errors," in *Proc. IEEE Int. Conf. Robotics and Automation*, Albuquerque, NM, 1997, pp. 1594–1599.

[20] Y. Tsumaki, H. Naruse, D. N. Nenchev, and M. Uchiyama, "Design of a compact 6-DOF haptic interface," in *Proc. IEEE Int. Conf. Robotics and Automation*, Leuven, Belgium, 1998, pp. 2580–2585.

[21] W. K. Yoon, S. Tachihara, Y. Tsumaki, and M. Uchiyama, "Evaluation of the different master device approaches for a model-based space teleoperation system," in *Proc. 10th Int. Conf. Advanced Robotics*, Budapest, Hungary, 2001, pp. 357–362.

[22] W. K. Yoon, Y. Tsumaki, and M. Uchiyama, "An experimental teleoperation system for dual-arm space robotics," *J. Robot. Mechatron.*, vol. 12, no. 4, pp. 378–384, 2000.

[23] M. Uchiyama, S. Kaneda, and K. Kitagaki, "A teleoperated force control system for space robots" (in Japanese), *J. Robot. Soc. Japan*, vol. 9, no. 7, pp. 849–856, 1991.